Effects of saturation and velocity-changing collisions on nonlinear mixing in resonant systems

S. Singh and G. S. Agarwal
School of Physics, University of Hyderabad Hyderabad, 500 134, India
(Received 9 April 1990)

We study the effects of velocity-changing collisions (VCC's) on nearly degenerate forward four-wave mixing (FWM) in the presence of a strong pump. The calculations include the effects of both VCC's and phase-interrupting collisions. Explicit calculations and results for FWM in two-level systems for the case of strong collisions are presented in the Doppler limit. Effects of saturation on VCC-induced narrowing and those of VCC's on strong-field-induced resonances are discussed in detail.

I. INTRODUCTION

In recent years the investigation of effects of velocity-changing collisions (VCC's) on four-wave mixing (FWM) signal line shapes has received considerable attention. Lam, Steel, and McFarlane[1] as early as 1982 reported the VCC-induced narrowing of the longitudinal relaxation linewidth which they experimentally observed using near-resonant FWM. Since then there have been a number of experiments carried out with nearly resonant fields. Lam, Steel, and McFarlane[2] generalized their previous studies to include the degeneracies of the ground state. Rothberg and Bloembergen[3,4] also made similar studies using the technique of FWM to study the effects of VCC's on collision induced Zeeman coherences between the degeneracies of the ground state of Na atom. These authors have also reported VCC-induced collisional narrowing[5] of the residual Doppler broadening (owing to a slight angle between the pump and probe beams) in the limit of large pump-atom detuning. Lam, Steel, and McFarlane[1] have discussed the effect of VCC's but did not include the residual Doppler broadening in their theoretical calculations. Gorlicki, Berman, and Khitrova[6] have presented a theoretical analysis including effects of VCC's and residual Doppler broadening.

Effects of a saturating pump field in degenerate[7] or nearly degenerate[8] four-wave mixing by homogeneously and Doppler broadened atomic vapors has been of great interest in recent years. However, the existing studies of saturation effects in FWM do not include VCC's. Most experiments and theoretical approaches that include VCC's are restricted to perturbation theory in the limit of nonsaturating fields. Study of the effects of VCC's when the incident fields are strong is seen to give rise to interesting effects. In their cw degenerate FWM (DFWM) experiments on the $D2$ line of atomic sodium Steel and McFarlane[9] demonstrated that VCC's lead to enhancement of FWM signals in the presence of a saturating pump.

It is the purpose of this work to investigate the effects of VCC's on nearly degenerate FWM in a system of two-level atoms when one of the incident fields is arbitrarily strong. A strong collision model is assumed to account for VCC's. The calculations are based on a simple and often applicable collision model in which collisions are both velocity changing and phase interrupting in their effect on level coherences. Level populations also change because of VCC's. The level width, collision rates, detunings, and the Rabi frequencies are restricted only by the impact approximation.

In Sec. II a scheme is presented for nonperturbative calculations of FWM signals for an arbitrarily strong incident pump field. A formal solution for the susceptibility for forward FWM geometry is obtained, valid to all orders in the incident pump amplitude and for arbitrary VCC's and dephasing collisional parameters. In Sec. III the FWM susceptibility $\chi^{(3)}$ is obtained in the near-resonant case (Doppler limit). This is an interesting limit and is important for many experimental situations. Numerical results for FWM signal line shapes are presented in Sec. IV. The effects of VCC's and pump intensity on the FWM signals are discussed. The results in the absence of VCC's are also given for comparison.

II. NONPERTURBATIVE CALCULATIONS FOR AN ARBITRARILY STRONG PUMP

Consider a vapor consisting of the two-level atoms interacting with a pump field $\mathbf{E}_l$ at frequency ω_l and a probe $\mathbf{E}_p$ at frequency ω_p given by

$$\mathbf{E}_j(\mathbf{r},t)=\boldsymbol{\varepsilon}_j\exp[i(\mathbf{k}_j\cdot\mathbf{r}-\omega_j t)]+\text{c.c.},\quad j=l,p\ . \tag{2.1}$$

The probe beam makes a small angle θ with the pump. The atomic energy separation between the upper ($|1\rangle$) and lower ($|2\rangle$) levels is $\hbar\omega_0$. The two-level system is closed, i.e., the lower level ($|2\rangle$) is the ground state and the upper level ($|1\rangle$) is the excited level that can decay radiatively only via spontaneous emission to the lower level at a rate γ.

These atoms are immersed in a buffer gas of foreign perturbers. The active atoms (i.e., that interact

significantly with the external fields) of the vapor undergo collisions with the perturber atoms (i.e., atoms that do not significantly interact with the external fields). The density of active atoms is assumed to be sufficiently low such that we consider only active-atom-perturber collisions. The atomic transition frequency ω_0 is shifted by kv as a result of atomic motion. Collisions with perturber atoms can cause a shift in the velocity v besides interrupting the phase of the dipole moment. To account for these collisions we make use of the impact approximation. In this approximation, the duration of a typical collision τ_c is assumed to be much less than the various time scales in the problem, i.e., $\tau_c^{-1} \gg$ atom-field detunings, Rabi frequencies, and collisional decay rates. Changes in velocity v occur through jumps from the value of v to another. The jump time is assumed to be instantaneous with regard to all other relevant time scales in the problem. Moreover, if we make the Markovian approximation,[10] then the value v following a jump depends at most on the value v' before the jump. We further assume the statistical independence of velocity-changing and phase-interrupting collisions.

In this framework the net effect of collisions is described by the inclusion of an additional term $[\partial\rho_{ij}/\partial t]_{\text{coll}}$ in the equations for density matrix elements[11] given by

$$\left[\frac{\partial\rho_{ij}(v,t)}{\partial t}\right]_{\text{coll}} = -\gamma_{\text{ph}}(v)\rho_{ij}(v,t) - \Gamma_{ij}(v)\rho_{ij}(v,t) + \int dv' W_{ij}(v'\to v)\rho_{ij}(v',t) , \quad (2.2)$$

where $\gamma_{\text{ph}}(v)$, $\Gamma_{ij}(v)$, and the kernel $W_{ij}(v'\to v)$ are well-defined quantum-mechanical functions.[12] The decay rate $\gamma_{\text{ph}}(v)$ occurs in pressure broadening theories involving phase-interrupting collisions, and it vanishes for $i=j$. The velocity changes of atoms during collision are accounted for by the collision kernel $W_{ij}(v'\to v)$ which couples different velocity classes. The decay rate Γ_{ij} is related to collision kernel via the relation

$$\Gamma_{ij}(v) = \int W_{ij}(v\to v')dv' . \quad (2.3)$$

Thus $\Gamma_{ij}(v)$ can be viewed as the decay that occurs due to collisions that remove active atoms from the velocity subclass v and $W_{ij}(v'\to v)$ as the contribution of other velocity subclasses to the subclass v. We can now write all the relevant density matrix equations. We will work in a frame rotating at the frequency of the pump field ω_l.

The equations for density-matrix elements for two-level atoms interacting with the external electromagnetic fields and undergoing collisions with perturber atoms are

$$\frac{d\tilde{\rho}_{12}(z,v,t)}{dt} = -[\Gamma_0(v)+\Gamma_{12}(v)+i(\Delta_l+k_l v)]\tilde{\rho}_{12}(z,v,t) - \frac{i}{2}[\alpha_l+\alpha_p e^{i(\kappa z-\delta t)}][\rho_{11}(z,v,t)-\rho_{22}(z,v,t)] + \int W_{12}(v'\to v)\tilde{\rho}_{12}(z,v',t)dv' , \quad (2.3a)$$

$$\frac{d\rho_{11}(z,v,t)}{dt} = -[\gamma+\Gamma_{11}(v)]\rho_{11}(z,v,t) + \frac{i}{2}[(\alpha_l+\alpha_p e^{i(\kappa z-\delta t)})\tilde{\rho}_{21}(z,v,t)-\text{c.c.}] + \int W_{11}(v'\to v)\tilde{\rho}_{11}(z,v',t)dv' , \quad (2.3b)$$

$$\frac{d\rho_{22}(z,v,t)}{dt} = \gamma\rho_{11}(z,v,t) - \Gamma_{22}(v)\rho_{22}(z,v,t) - \frac{i}{2}[(\alpha_l+\alpha_p e^{i(\kappa z-\delta t)})\tilde{\rho}_{21}(z,v,t)-\text{c.c.}] + \int dv' W_{22}(v'\to v)\rho_{11}(z,v',t) , \quad (2.3c)$$

$$\tilde{\rho}_{21}(z,v,t) = [\tilde{\rho}_{12}(z,v,t)]^* , \quad (2.3d)$$

where we have made the transformation

$$\rho_{12}(z,v,t) = \tilde{\rho}_{12} e^{i(k_l z-\omega_l t)} . \quad (2.3e)$$

Here $\Gamma_0(v)$ $[=\gamma/2+\gamma_{\text{ph}}(v)]$ is the usual decay rate associated with off-diagonal matrix elements, Δ_l $(=\omega_0-\omega_l)$ is the detuning of pump frequency from atomic resonance, δ $(=\omega_p-\omega_l)$ is the probe-pump detuning, $\kappa=k_p-k_l$, and α_j $(=2\mathbf{d}\cdot\boldsymbol{\varepsilon}_j/\hbar)$; $j=l,p$, is the Rabi frequency associated with the field $\mathbf{E}_j$.

The exact solution of Eqs. (2.3) for an arbitrary kernel is tedious and requires extensive numerical computation. Exact solution are however possible for various limiting forms of the kernel. Of particle interest and most often applicable is the so-called strong-collision model. Here rapid thermalization of velocity distribution of active atom occurs after collisions. A single collision, on the average, thermalizes the velocity distribution. The collision kernel is given by

$$W_{ij}(v'\to v) = \Gamma_{ij}M(v) , \quad (2.4)$$

where $M(v)$ is the Maxwellian velocity distribution given by

$$M(v) = (v_{\text{th}}\sqrt{\pi})^{-1}\exp(-v^2/v_{\text{th}}^2) . \quad (2.5)$$

Substituting (2.4) in Eq. (2.3), for the strong collision model, the equations for density matrix elements can be recast in a different form:

$$\frac{d\psi(z,v,t)}{dt} = -A(v,t)\psi(z,v,t) + B(v)M(v)\int \psi(z,v',t)dv' + C(z,v,t)\psi(z,v,t) \ . \tag{2.6}$$

where

$$\psi(z,v,t) = \begin{bmatrix} \tilde{\rho}_{12}(z,v,t) \\ \tilde{\rho}_{21}(z,v,t) \\ [\rho_{11}(z,t)-\rho_{22}(z,v,t)] \\ [\rho_{11}(z,v,t)+\rho_{22}(z,v,t)] \end{bmatrix} , \tag{2.7a}$$

$$A(v,t) = \begin{bmatrix} \Gamma_0+\Gamma_{12}+i(\Delta_l+k_l v) & 0 & i\alpha_l/2 & 0 \\ 0 & \Gamma_0+\Gamma_{12}-i(\Delta_l+k_l v) & -i\alpha_l^*/2 & 0 \\ i\alpha_l^* & -i\alpha_l & \gamma+a & \gamma+b \\ 0 & 0 & 0 & a \end{bmatrix} , \tag{2.7b}$$

and the nonvanishing elements of $B(v)$ and $C(z,v,t)$ are given by

$$\begin{aligned} &B_{11}=B_{22}=\Gamma_{12}, \quad B_{33}=B_{44}=a, \quad B_{34}=B_{43}=b \ , \\ &2C_{13}=-2C_{23}^*=C_{31}^*=-C_{32}=-\alpha_p e^{i(\kappa z-\delta t)} \ , \end{aligned} \tag{2.7c}$$

and

$$a=\tfrac{1}{2}[\Gamma_{11}(v)+\Gamma_{22}(v)], \quad b=\tfrac{1}{2}[\Gamma_{11}(v)-\Gamma_{22}(v)] \ . \tag{2.8}$$

We will obtain signals to all orders in the pump field but to first order in the probe field. For this purpose we express ψ as

$$\psi=\psi^{(0)}+\psi^{(1)}+\cdots \ , \tag{2.9}$$

where the zeroth-order solution $\psi^{(0)}$ corresponds to all orders in the pump-field amplitude α_l. The first-order solution $\psi^{(1)}$ is valid to all orders in pump amplitude α_l but only to leading order in the probe amplitude α_p. This assumption is valid as usually, the probe is nonsaturating. From (2.9) and (2.6) we find the conservation equation to zeroth order in the probe field

$$\begin{aligned} \frac{d}{dt}[\rho_{11}^{(0)}(z,v,t)+\rho_{22}^{(0)}(v,t)] &= -b[\rho_{11}^{(0)}(v,t)-\rho_{22}^{(0)}(v,t)]+bM(v)\int dv'[\rho_{11}^{(0)}(v',t)-\rho_{22}^{(0)}(v',t)] \\ &\quad -a[\rho_{11}^{(0)}(v,t)+\rho_{22}^{(0)}(v,t)]+aM(v)\int dv'[\rho_{11}^{(0)}(v',t)+\rho_{22}^{(0)}(v',t)] \ , \end{aligned} \tag{2.10}$$

which implies that

$$\int dv[\rho_{11}^{(0)}(v,t)+\rho_{22}^{(0)}(v,t)]=\text{const}=1 \ .$$

Thus the equation for zeroth-order quantities are obtained as

$$\frac{d\psi^{(0)}(v,t)}{dt} = -A(v)\psi^{(0)}(v,t)+B^{(0)}(v)M(v)\int dv'\psi^{(0)}(v',t)+D^{(0)}(v) \ , \tag{2.11}$$

where nonvanishing elements of $B^{(0)}$ and $D^{(0)}$ are

$$\begin{aligned} &B_{11}^{(0)}=B_{22}^{(0)}=\Gamma_{12}, \quad B_{33}^{(0)}=B_{44}^{(0)}=a \ , \\ &D_{34}^{(0)}=D_{43}^{(0)}=b \ . \end{aligned} \tag{2.12}$$

The first-order quantities $\psi^{(1)}$ are obtained from the solution of the equation

$$\begin{aligned} \frac{d\psi^{(1)}(z,v,t)}{dt} &= -A(v,t)\psi^{(1)}(z,v,t) \\ &\quad +B(v)M(v)\int \psi^{(1)}(z,v',t)dv' \\ &\quad +iC(z,t)\psi^{(0)}(v,t) \ . \end{aligned} \tag{2.13}$$

We are interested in the steady-state response of the system. In particular we want to determine the first-order response at frequency $2\omega_l-\omega_p$ which provides the nonlinear polarization giving rise to four-wave mixing. The Fourier decomposition of the first order quantities $\psi^{(1)}$ can be done as follows:

$$\psi^{(1)}=\psi_- e^{i(\kappa z-\delta t)}+\psi_+ e^{-i(\kappa z-\delta t)} \ . \tag{2.14}$$

From Eqs. (2.14), (2.7), and (2.13), the equations for slowly varying quantities ψ_+ is obtained as

$$\begin{aligned} \frac{\partial\psi_+(v,t)}{\partial t} &= -A_+(v)\psi_+(v,t) \\ &\quad +BM(v)\int \psi_+(v',t)dv'+C_+\psi^{(0)}(v,t) \ , \end{aligned} \tag{2.15}$$

where $A_+(v)$ is obtained from $A(v,t)$ by replacing A_{11} and A_{22} by $\Gamma_0+\Gamma_{12}+i(\Delta_s+k_s v)$ and $\Gamma_0+\Gamma_{12}-i(\Delta_p+k_p v)$, respectively, and where the nonvanishing elements of C_+ are

$$2(C_+)_{23}=-(C_+)_{31}=i\alpha_p^*$$

and

$$\Delta_s=\Delta_l+\delta,\quad k_s=k_l-\kappa\ ,$$
$$\Delta_p=\Delta_l-\delta,\quad k_p=k_l+\kappa\ . \tag{2.16}$$

For simplicity we will ignore the velocity dependence of collisional parameters $\gamma_{\rm ph}$, Γ_{ij}, etc. This is justified as these generally are slowly varying functions of v. To determine the steady-state characteristics, Eqs. (2.15) and (2.11) can be solved algebraically by setting the left-hand side equal to zero. From (2.14), (2.9), (2.7), and (2.3), we find that the steady-state response at frequency $2\omega_l-\omega_p$ is given by $(\psi_+)_1$, the first element of the column matrix ψ_+. With this the induced macroscopic nonlinear polarization at frequency ω_s $(=2\omega_l-\omega_p)$ and a wave vector $k_s(=2k_l-k_p)$ is

$$P=Nd_{21}\int dv(\psi_+(v))_1 e^{i(k_s z-\omega_s t)}+\text{c.c.}\ , \tag{2.17}$$

where N is the atomic density of the vapor. Equation (2.17) yields the steady-state four-wave mixing susceptibility of the vapor valid for arbitrary pump intensities and to the leading order in probe field.

From Eq. (2.15) we find that a formal solution for velocity averaged steady-state first-order quantities ψ_+ is

$$\int dv\ \psi_+(v)=\left[I-\int dv' M(v')A_+^{-1}(v')B\right]^{-1}\times\int dv\ A_+^{-1}(v)C_+\psi^{(0)}(v)\ , \tag{2.18}$$

with

$$\psi^{(0)}(v)=A^{-1}(v)B^{(0)}(v)M(v)\times\left[I-\int dv'' M(v'')A^{-1}(v'')B^{(0)}\right]^{-1}\times\int dv' A^{-1}(v')D^{(0)}+A^{-1}(v)D^{(0)}\ , \tag{2.19}$$

where I is a unit matrix of dimension 4. Thus from (2.17), (2.18), (2.19), and (2.16), the four-wave mixing susceptibility $\chi(\omega_l,\omega_l,-\omega_p)$ can be calculated. Calculations of FWM susceptibility in the Doppler limit and for small pump-probe separation angle is performed in Sec. III.

The FWM signal is proportional to S defined by

$$S=\left|\int dv(\psi_+(v))_1\right|^2\ . \tag{2.20}$$

III. CALCULATION OF FWM SIGNALS IN DOPPLER LIMIT

In Sec. II we have seen that it is possible to obtain exact analytical expression for the FWM signal valid for arbitrary pump intensities, collisional parameters and detunings. A solution for polarization [Eq. (2.17)] however, in its exact form is virtually intractable. A considerable simplification is made in the grazing angle approximation in which the angle between pump and probe beams is very small. We further restrict the following analysis to the Doppler limit. In this limit the velocity integration becomes analytically tractable. The Doppler limit is interesting as well as important for many experimental situations.

In the Doppler limit, the Doppler width is large compared to the collisional parameters, detunings, and Rabi frequency of the saturating pump α_l. The first condition is satisfied for low perturber pressures, but the last condition sets an upper limit on the intensity of the saturating pump $\alpha_l \ll kv_{\rm th}$. In the Doppler limit, the Maxwell-Boltzmann factor $\exp(-v^2/v_{\rm th}^2)$ can be assumed constant over the range of integration. The velocity integration of integrands in Eq. (2.17) may then be carried out by closing the integration contour at $v=\pm\infty$ in the appropriate part of the complex plane (upper- or lower-half plane) and using the residue theorem. The integration consists of locating the poles of the integrands in the expression for susceptibility $\chi^{(3)}$.

In the grazing angle approximation, the terms like $(\kappa v-\delta)$ can be approximated as $\delta(v/c-1)\simeq-\delta$ as typically $v\sim 10^4$ cm sec^{-1} and hence $v/c\ll 1$. Also since $\Gamma_{12}\ll kv_{\rm th}$, the terms with Γ_{12} dependence can be ignored in the expression for P [Eq. (2.17)]. With these approximations, the expression for P is notably simplified. The formal expression for $\chi^{(3)}$ is then reduced to

$$\chi^{(3)}(\omega_l,\omega_l,-\omega_p)\simeq-\frac{i}{2}Nd\alpha_l^2\gamma\left[1-\left[a-b\frac{\gamma+b}{a}\right]\langle\mathcal{R}(v)\rangle\right]^{-1}\times\Big\{\langle\mathcal{L}(v)\mathcal{R}(v)C(k_s v+\Delta_s,\Gamma_0+\Gamma_{12})C(-k_p v-\Delta_p,\Gamma_0+\Gamma_{12})\rangle$$
$$+\langle\mathcal{L}(v)\mathcal{R}(v)C(k_s v+\Delta_s,\Gamma_0+\Gamma_{12})C(k_l v+\Delta_l,\Gamma_0+\Gamma_{12})\rangle$$
$$+\left[1-\left[a-\frac{b(\gamma+b)}{a+i\delta}\right]\mathcal{L}(v)\right]^{-1}\left[a-\frac{b(\gamma+b)}{a+i\delta}\right]\langle\mathcal{L}(v)C(k_s v+\Delta_s,\Gamma_0+\Gamma_{12})\rangle$$
$$\times[\langle\mathcal{L}(v)\mathcal{R}(v)C(-k_p v-\Delta_p,\Gamma_0+\Gamma_{12})\rangle+\langle\mathcal{L}(v)\mathcal{R}(v)C(k_l v+\Delta_l,\Gamma_0+\Gamma_{12})\rangle]\Big\}\ , \tag{3.1}$$

where

$$\mathcal{R}(v)=\left[\gamma+a-\frac{b}{a}(\gamma+b)+\alpha_l^2(\Gamma_0+\Gamma_{12})|C(k_l v+\Delta_l,\Gamma_0+\Gamma_{12})|^2\right]^{-1}$$

and

$$\mathcal{L}(v)=[\gamma+a+i\delta-b(\gamma+b)C(\delta,a)+\alpha_l^2(\Gamma_0+\Gamma_{12}+i\delta)C(k_s v+\Delta_s,\Gamma_0+\Gamma_{12})C(-k_p v-\Delta_p,\Gamma_0+\Gamma_{12})]^{-1} . \tag{3.2}$$

In the above, the angular bracket $\langle\ \rangle$ denotes average over a Maxwellian distribution $M(v)$ and $C(x,y)$ denotes a complex Lorentzian

$$C(x,y)=\frac{1}{y+ix} . \tag{3.3}$$

We now have to locate the poles of the integrals in the above expression for $\chi^{(3)}$. The denominator of $\chi^{(3)}$ contains the intensity-dependent factor

$$[\Gamma_0+\Gamma_{12}-i(\Delta_l-\delta+v)][\Gamma_0+\Gamma_{12}+i(\Delta_l+\delta+v)]+\alpha_l^2\frac{(\Gamma_0+\Gamma_{12}+i\delta)(a+i\delta)}{(a+b+\gamma+i\delta)(a-b+i\delta)} . \tag{3.4}$$

For $\alpha_l=0$ it has two poles; one located in the complex upper and the other in the lower-half plane. For $\alpha_l\neq 0$, the above term can be factorized as

$$(v+\Delta_l+\sqrt{\xi}-i\sqrt{\eta})(v+\Delta_l-\sqrt{\xi}+i\sqrt{\eta}) ,$$

with

$$\sqrt{\eta}+i\sqrt{\xi}=(\Gamma_0+\Gamma_{12}+i\delta)\left[1+\alpha_l^2\frac{a+i\delta}{(\Gamma_0+\Gamma_{12}+i\delta)(a+b+\gamma+i\delta)(a-b+i\delta)}\right]^{1/2} , \tag{3.5}$$

which shows that one pole is in the upper-half plane and the other in the lower plane. The factorization of other intensity-dependent factor in the denominator is straightforward. For example, consider the denominator

$$[\Gamma_0+\Gamma_{12}+i(\Delta_l+v)][\Gamma_0+\Gamma_{12}-i(\Delta_l+v)]+\alpha_l^2\frac{a(\Gamma_0+\Gamma_{12})}{(a-b)(a+b+\gamma)}=(v+\Delta_l+i\sqrt{\beta})(v+\Delta_l-i\sqrt{\beta}) ,$$

where

$$\sqrt{\beta}=(\Gamma_0+\Gamma_{12})\left[1+\alpha_l^2\frac{a}{(\Gamma_0+\Gamma_{12})(a+b+\gamma)(a-b)}\right]^{1/2} . \tag{3.6}$$

With these, the evaluation of integrals in Eq. (3.1) using calculus of residues is straightforward. The form of $\chi^{(3)}$ thus obtained is

$$\chi^{(3)}(\omega_l,\omega_l,-\omega_p)\simeq-\frac{i}{2}Nd\alpha_l^2\frac{\sqrt{\pi}}{kv_{\rm th}}\frac{\gamma}{\tilde{\gamma}(\alpha)}\frac{(\Gamma_0+\Gamma_{12})}{\sqrt{\beta}}\frac{2(\Gamma_0+\Gamma_{12})+i\delta}{(\Gamma_0+\Gamma_{12}+i\delta)^{1/2}}\mathcal{D}_1^{-1/2}(\alpha)\mathcal{D}_2^{-1}(\alpha)$$
$$\times\left[(a+i\delta)+\frac{\sqrt{\pi}}{kv_{\rm th}}\frac{a}{\mathcal{D}_3(\alpha)}(\Gamma_0+\Gamma_{12}+i\delta)\left[a-\frac{b}{a}(\gamma+b)+i\delta\right]\left[\mathcal{D}_1^{1/2}(0)+\frac{\sqrt{\beta}}{(\Gamma_0+\Gamma_{12})}\mathcal{D}_1^{1/2}(\alpha)\right]\right] , \tag{3.7}$$

where

$$\tilde{\gamma}(\alpha)=\gamma+\alpha_l^2\frac{\sqrt{\pi}}{kv_{\rm th}}\frac{a-b(\gamma+b)/a}{\gamma+a-b(\gamma+b)/a}\frac{\Gamma_0+\Gamma_{12}}{\sqrt{\beta}} ,$$

$$\mathcal{D}_1(\alpha)=(\Gamma_0+\Gamma_{12}+i\delta)(a-b+i\delta)(a+b+\gamma+i\delta)+\alpha_l^2(a+i\delta) ,$$

$$\mathcal{D}_2(\alpha)=(\Gamma_0+\Gamma_{12}+i\delta)^{1/2}\mathcal{D}_1^{1/2}(\alpha)+\sqrt{\beta}(a+b+\gamma+i\delta)^{1/2}(a-b+i\delta)^{1/2} , \tag{3.8}$$

$$\mathcal{D}_3(\alpha)=(\gamma+i\delta)\mathcal{D}_1^{1/2}(\alpha)+\frac{\sqrt{\pi}}{kv_{\rm th}}\alpha_l^2\frac{[a(a+i\delta)-b(\gamma+b)](\Gamma_0+\Gamma_{12}+i\delta)^{1/2}}{(a+b+\gamma+i\delta)^{1/2}(a-b+i\delta)^{1/2}} .$$

If all the VCC's effects are ignored, then the above expression after setting $a=b=0$ reduces to

$$\chi(\omega_l,\omega_l,-\omega_p)\simeq-\frac{i}{2}Nd\alpha_l^2\frac{\sqrt{\pi}}{kv_{\rm th}}\frac{\Gamma_0}{\sqrt{\phi}}\times\frac{2\Gamma_0+i\delta}{(\Gamma_0+i\delta)^{1/2}}Z_1^{-1/2}(\alpha)Z_2^{-1}(\alpha)\ , \tag{3.9}$$

where

$$\begin{aligned}Z_1(\alpha)&=(\Gamma_0+i\delta)(\gamma+i\delta)+\alpha_l^2\ ,\\ Z_2(\alpha)&=(\Gamma_0+i\delta)^{1/2}[(\Gamma_0+i\delta)(\gamma+i\delta)+\alpha_l^2]^{1/2}\\ &\quad+\sqrt{\phi}(\gamma+i\delta)^{1/2}\ ,\\ \sqrt{\phi}&=\Gamma_0\left[1+\frac{\alpha_l^2}{\gamma\Gamma_0}\right]^{1/2}.\end{aligned} \tag{3.10}$$

Expansion of Eq. (3.7) in power of α_l^2 and retaining only the leading terms in α_l^2 leads to the perturbation theory result[13] for forward four-wave mixing.

IV. FOUR-WAVE MIXING SIGNALS: NUMERICAL CALCULATIONS

In this section, we present the FWM signals calculated numerically using (3.7). The signals are displayed as a function of the probe-pump detuning δ for a range of collisional parameters $\gamma_{\rm ph}$, Γ_{ij} and pump amplitude α_l within the Doppler limit. Results in the absence of VCC's are also presented for comparison. We also discuss the case when the collision kernels for upper and lower states are identical, i.e., the case when $\Gamma_{11}=\Gamma_{22}$. The modifications in FWM signals due to VCC's in the presence of a high pump field are discussed in detail.

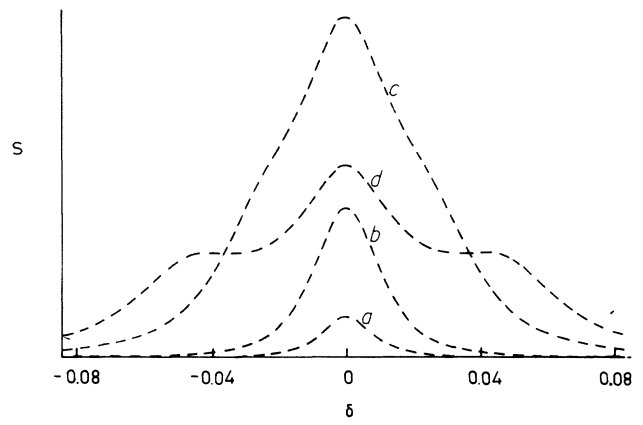

FIG. 1. Four-wave mixing (FWM) signals S as a function of probe-pump detuning δ, for various values of the pump amplitude α_l, and for the moderate collisional dephasing parameter $\gamma_{\rm ph}$ $(=2\gamma)$, in the absence of VCC's, i.e., $\Gamma_{22}=\Gamma_{11}=\Gamma_{12}=0$. Curves a, b, c, and d correspond to the values of $\alpha_l=0.1\gamma$, γ, 3γ, and 5γ, respectively. The magnitude of signal shown for curve a is 10^3 times the actual value. All the parameters are scaled in terms of the Doppler width γ_D $(=100\gamma)$. The magnitude of the signal on the y axis for all the other curves in the figure are normalized with respect to the maximum of the highest peak in that particular figure.

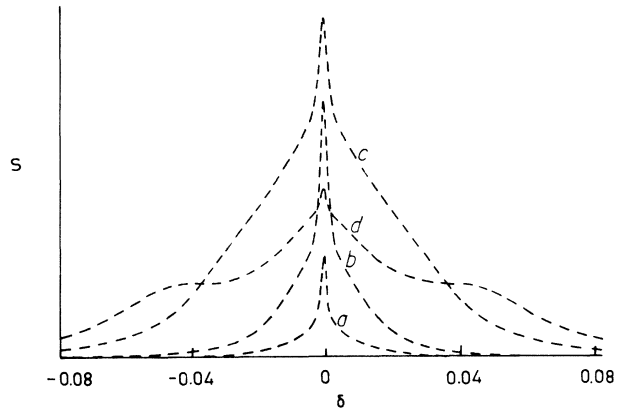

FIG. 2. FWM signals S as a function of the probe-pump detuning δ, for various values of pump amplitude α_l and for moderate values of $\gamma_{\rm ph}$ $(=2\gamma)$, when VCC's parameter is small; Γ_{22} $(=0.1\gamma)$. Curves a, b, c, and d correspond to $\alpha_l=0.1\gamma$, γ, 3γ, and 5γ, respectively. The magnitude of the signal for curve a shown in the figure is 10^3 times the actual value. Because in general, for optical transitions, $\Gamma_{11}>\Gamma_{22}$ we have made the choice of $\Gamma_{11}=3\Gamma_{22}$ and $\Gamma_{12}=\Gamma_{22}$. The normalization on the y axis and the rest are the same as in Fig. 1.

In Figs. 1, 2, and 3 FWM signals are shown as a function of probe-pump detuning δ for various values of the pump amplitude α_l, for moderate values of the collisional dephasing parameters $\gamma_{\rm ph}(=2\gamma)$, and for small VCC's parameter $\Gamma_{22}(\ll\gamma)$. Curves a of these figures show the results as obtained by a perturbation theory when $\alpha_l\ll\gamma$. In the absence of VCC's, the system is closed,[1,6] i.e., the only population decay that occurs is via spontaneous emission from the upper to the lower state. As

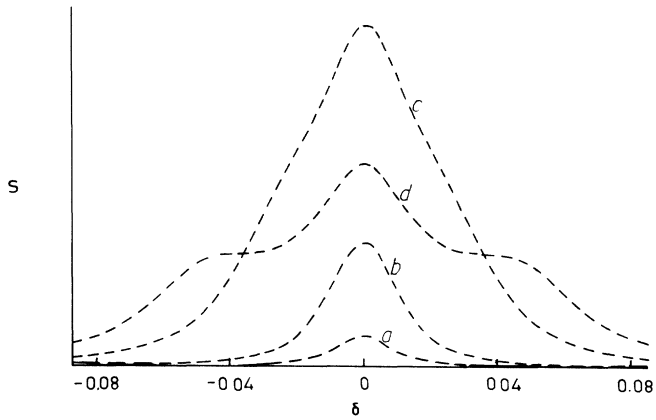

FIG. 3. FWM signals S as a function of δ for various values of α_l and for moderate $\gamma_{\rm ph}$ $(=2\gamma)$ when Γ_{22} $(=0.1\gamma)$ is small. Curves a, b, c, and d correspond to the values of $\alpha_l=0.1\gamma$, γ, 3γ, and 5γ, respectively. The magnitude of signal shown for curve a is 10^3 times the actual value. This figure corresponds to the case when collision kernels are identical, i.e., $\Gamma_{11}=\Gamma_{22}=\Gamma_{12}$. The normalization on the y axis and the rest are the same as in Fig. 1.

observed from curve *a* of Fig. 1, a single resonance centered around $\omega_l=\omega_p$ exists, the width of which is governed by the natural line width γ. In the presence of VCC's extreme narrowing of this resonance occurs (see curve *a* of Fig. 2) when $\Gamma_{11}\neq\Gamma_{22}$ (as is true for most optical transitions).[6] For $\Gamma_{22}\ll\gamma$, the width of the resonance at $\omega_l=\omega_p$ is governed by the VCC's induced ground-state decay rate Γ_{22}.[13] VCC's provide a mechanism for opening the system[1,6] by causing decay of the upper- and lower-level populations. When the collision kernels for upper and lower levels are dissimilar (as is the case for most optical transitions), a very narrow resonance at $\omega_l=\omega_p$ appears. One can see from the perturbation theory result for nonsaturating fields that this is so because the behavior near $\delta=0$ is determined by several resonances with differing widths. If these widths differ very much from one another then the behavior would be dominated by the resonance with the least width. The resonances[14] characterized by ground-state decay rates occur because of a difference in the excited- and ground-state collision kernels. For identical kernels, i.e., when $\Gamma_{11}=\Gamma_{22}$, the system remains closed in the sense that the width of the peak at $\omega_l=\omega_p$ is governed by γ as in the case of a closed system in the absence of VCC's. This can be seen from curve *a* of Fig. 3. With increase in pump amplitude α_l, the structure at $\omega_l=\omega_p$ broadens. As α_l increases further, curve *d* in Figs. 1, 2, and 3 shows that the singlet structure goes over to a triplet. Two partially resolved peaks (ac Stark resonances) begin to appear on either side of the power broadened central peak. This can be seen from the denominators such as $\mathcal{D}_1(\alpha)$ and $\mathcal{Z}_1(\alpha)$ occurring in Eqs. (3.7) and (3.9), respectively. As discussed above, for the nonsaturating pump α_l the denominator $\mathcal{D}_1(\alpha)$ predicts a narrow resonance at $\delta=0$ with a width Γ_{22} $(=a-b)$. With an increase in the pump amplitude α_l this resonance shows power broadening. For the saturating pump and in the limit $a-b+i\delta\approx a+i\delta$, from $\mathcal{D}_1(\alpha)$ and (2.8) we find the position and width of the ac Stark resonances as

$$i\delta=-\tfrac{1}{2}[(\gamma+\Gamma_{11})+(\Gamma_0+\Gamma_{12})] \pm\left[\left[\frac{(\gamma+\Gamma_{11})-(\Gamma_0+\Gamma_{12})}{2}\right]^2-\alpha_l^2\right]^{1/2}. \quad (4.1)$$

When α_l is much larger, $\alpha_l^2\gg(\gamma+\Gamma_{11}-\Gamma_0-\Gamma_{12})^2/4$, these resonances will be fully resolved at $\pm\alpha_l$ with a width $(\gamma+\Gamma_{11}+\Gamma_0+\Gamma_{12})/2$. Thus we find that the VCC-induced narrowing of the peak at $\omega_l=\omega_p$ begins to disappear with increasing pump intensity and the width of the ac Stark resonances are modified by VCC's. From Figs. 1–3 we observe that the FWM signals saturates as $\alpha_l\to\Gamma_0+\Gamma_{12}(\sim 2.5\gamma)$.

It is clear that the saturation of FWM signals with an increase in the pump amplitude α_l is affected by the presence of VCC's. The behavior of FWM signals is shown in Fig. 4 for the same value of $\gamma_{ph}(=2\gamma)$ as in the previous figures, but for a larger VCC rate $\Gamma_{22}=5\gamma$. It should be noted that for large VCC's, the system is effectively like a closed system, i.e., the narrowing of the structure at $\omega_l=\omega_p$ vanishes and the width is governed by the natural linewidth γ.

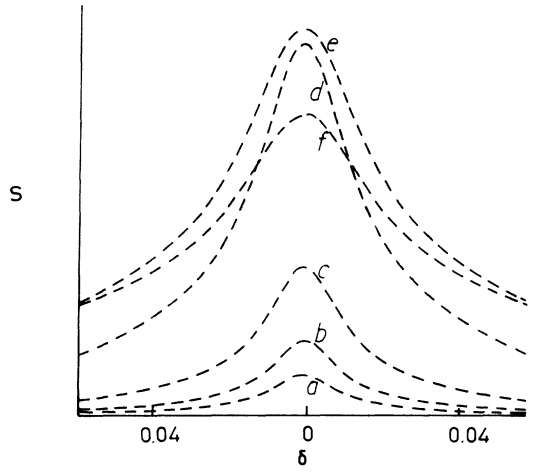

FIG. 4. FWM signals S as a function of the probe-pump detuning δ for various values of pump amplitude α_l, for the moderate collisional dephasing parameter γ_{ph} $(=2\gamma)$ and a higher VCC parameter Γ_{22} $(=5\gamma)$. Curves *a*, *b*, *c*, *d*, *e*, and *f* correspond to pump amplitudes $\alpha_l=0.1\gamma$, γ, 3γ, 5γ, 8γ, and 10γ, respectively. The magnitude of the signals shown in the figure for curves *a* and *b* are 10^5 and 20 times the actual values, respectively. This figure corresponds to the case when $\Gamma_{11}=3\Gamma_{22}$. FWM signals exhibit similar behavior in the other case when $\Gamma_{11}=\Gamma_{22}=\Gamma_{12}$, and hence the results are not presented. The normalization on the *y* axis and the rest are the same as in Fig. 1.

In Fig. 5, the effects of VCC's on FWM signals is shown for moderate value of pump amplitude α_l $(=5\gamma)$, and moderate γ_{ph} $(=2\gamma)$. Curve *b* shows that for large α_l, in the absence of VCC's, the signal structure is a triplet with a broad peak at $\delta=0$ and two ac Stark reso-

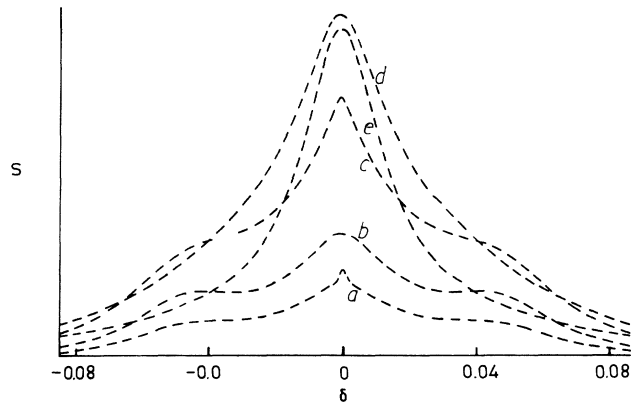

FIG. 5. The effect of increasing VCC parameters Γ_{22} on FWM signals S for a moderate value of collisional dephasing parameter γ_{ph} $(=2\gamma)$ and a higher value of the pump amplitude α_l $(=5\gamma)$. Curve *b* is the result in the absence of VCC's $(\Gamma_{11}=\Gamma_{22}=\Gamma_{12}=0)$. Curves *a*, *c*, *d*, and *e* correspond to the values of VCC parameters $\Gamma_{22}=0.1\gamma$, 0.3γ, 5γ, and 7γ, respectively. The magnitude of signal shown in the figure for curve *c* is 2 times the actual values. This figure is for the case when $\Gamma_{11}=3\Gamma_{22}$. The normalization on the *y* axis and the rest are the same as in Fig. 1. Note that with increase in Γ_{22}, the side peaks are broadened. The narrowing of curve *e* is due to further suppression of unresolved side peaks at higher values of Γ_{22}.

nances at $\pm\alpha_l$. In the absence of VCC's, the width of the side peaks is given according to (4.1) with $\Gamma_{11}=\Gamma_{12}=0$. With the appearance of VCC's (curve *a*), a spike develops in the central peak and the side peaks broaden. The broadening of the ac Stark resonances results from the increased decay in the system due to VCC's. This can be understood by looking at the denominators in Eq. (3.7) that give rise to the ac Stark resonances, in which the decay rates γ and Γ_0 are modified in the presence of VCC's to $\gamma+\Gamma_{11}$ and $\Gamma_0+\Gamma_{12}$, respectively. A remarkable feature that emerges is, the considerable enhancement of FWM signals[9] due to VCC's in the presence of high field. At lower rates of VCC's, the FWM signal for the case $\Gamma_{11}\neq\Gamma_{22}$ initially decreases compared to the case when VCC's are absent. With a further increase in the VCC parameter within the Doppler limit, the magnitude of the signal increases. This is because at lower perturber pressures VCC's remove the atoms from the frequency holes created by exciting fields (leading to increased decay rates), but with negligible replenishment of holes. However with increasing pressure, atoms in nonresonant velocity subclasses can be shifted into resonance if they experience appropriate velocity-changing collisions. Hence collisional redistribution occurs over a wider range of velocity groups and more and more atoms participate in interaction with the fields, thus giving rise to enhancement of signals. The signals saturate as $\Gamma_0+\Gamma_{12}$ approaches α_l and then decrease.

Figure 6 shows the effect of VCC's and pump field on FWM signals when $\gamma_{\rm ph}$ $(=8\gamma)$ is large and small Γ_{22} $(=\gamma/10)$. For small α_l, the structure at $\delta=0$ is extremely narrow with a width of Γ_{22}. As the pump amplitude α_l increases, this structure is seen as a spike on a broad pedestal that occurs due to power broadening. When $\alpha_l=5\gamma$, the spike vanishes and a single broad peak at $\omega_l=\omega_p$ results, as the side peaks are not resolved for this high rate of $\gamma_{\rm ph}$. At large values of α_l $(=8\gamma)$ a dip appears in the line center of the power-broadened peak at $\omega_l=\omega_p$, the depth of which increases with further increase in α_l. This dip vanishes in the absence of VCC's. The appearance of this is associated with the difference in collision kernels for upper and lower states. When $\Gamma_{11}=\Gamma_{22}$, the dip vanishes.

In conclusion, we have studied the effects of VCC's on FWM in the presence of a saturating pump. The redistributions of atomic velocities due to velocity-changing collisions by foreign perturbers in the presence of a strong field gives rise to interesting effects such as enhancement of signals and a dip in the line center. The present theory is restricted to strong-collision model for VCC's. Further generalization of the theory is possible. One can, for example introduce Keilson-Storer collision kernel[15] which will enable one to study the effects of VCC's in the more realistic intermediate regimes.

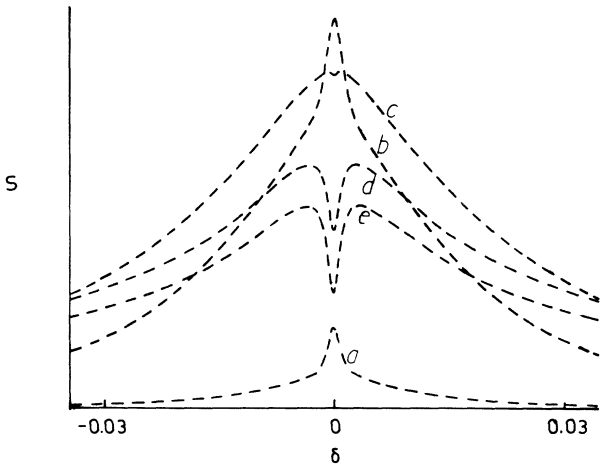

FIG. 6. FWM signals S as a function of δ for various values of pump amplitude α_l for large collisional dephasing parameter $\gamma_{\rm ph}$ $(=8\gamma)$ and small VCC's parameter Γ_{22} $(=0.1\gamma)$. Curve *a*, *b*, *c*, *d*, and *e* correspond to the values of $\alpha_l=0.1\gamma$, 3γ, 5γ, 8γ, and 10γ, respectively. The magnitude of signal shown in the figure, for curve *a* is 10^4 times the actual value. These results are for the case when $\Gamma_{11}=3\Gamma_{22}$, $\Gamma_{12}=\Gamma_{22}$. Note that the saturation of transition in the presence of VCC's lead to a dip at the line center provided that $\Gamma_{11}\neq\Gamma_{22}\neq0$. The normalization on the *y* axis and the rest are the same as in Fig. 1.

ACKNOWLEDGMENTS

S.S. is grateful to the Council for Scientific and Industrial Research (Government of India) and the Department of Science and Technology (Government of India), for partial support during the course of this research.

[1]J. F. Lam, D. G. Steel, and R. A. McFarlane, Phys. Rev. Lett. **49**, 1628 (1982).
[2]J. F. Lam, D. G. Steel, and R. A. McFarlane, Phys. Rev. Lett. **56**, 1679 (1986).
[3]L. J. Rothberg and N. Bloembergen, Phys. Rev. A **30**, 820 (1983).
[4]L. J. Rothberg, in *Progress in Optics*, edited by E. Wolf (North-Holland, Amsterdam, 1987), Vol. 24.
[5]L. J. Rothberg and N. Bloembergen, Phys. Rev. A **30**, 2327 (1984).
[6]M. Gorlicki, P. R. Berman, and G. Khitrova, Phys. Rev. A **37**, 4340 (1988).
[7]M. Ducloy, F. A. M. de Oliveira, and D. Bloch, Phys. Rev. A **32**, 1614 (1985); B. Kleinmann, F. Trehin, M. Pinard, and G. Grynberg, J. Opt. Soc. Am. B **2**, 704 (1985).
[8]M. Pinard, P. Verkerk, and G. Grynberg, Phys. Rev. A **35**, 4679 (1987); F. A. M. de Oliveira, C. B. de Araujo, and J. R. R. Leite, Phys. Rev. A **38**, 5688 (1988).
[9]D. G. Steel and R. A. McFarlane, Phys. Rev. A **27**, 1217 (1983).
[10]P. R. Berman, J. Opt. Soc. Am. B **3**, 572 (1986).
[11]P. R. Berman, J. Opt. Soc. Am. B **3**, 564 (1986).
[12]P. R. Berman, in *New Trends in Atomic Physics*, edited by G. Grynberg and R. Stora (North-Holland, Amsterdam, 1984),

pp. 453–514 and references therein.
[13]S. Singh, and G. S. Agarwal, J. Opt. Soc. Am. B **5**, 2515 (1988).
[14]G. Khitrova, P. R. Berman, and M. Sargent III, J. Opt. Soc. Am. B **5**, 160 (1988). These authors predict an extra resonance at $\delta=0$ in pump-probe absorption spectroscopy when the upper and lower levels of a two-level system decay at different rates to a reservoir.
[15]J. Keilson and K. E. Storer, Q. Appl. Math. **10**, 243 (1952).